

## Celecoxib Inhibits Meningioma Tumor Growth in a Mouse Xenograft Model

Brian T. Ragel, M.D.,<sup>1,2</sup> Randy L. Jensen, M.D., Ph.D.,<sup>1,2</sup> David L. Gillespie, Ph.D.,<sup>2</sup>  
Stephen M. Prescott, M.D.,<sup>2</sup> William T. Couldwell, M.D., Ph.D.<sup>1,2</sup>

<sup>1</sup>Department of Neurosurgery and <sup>2</sup>Huntsman Cancer Institute, University of Utah, Salt  
Lake City, Utah

Corresponding author:

William T. Couldwell, MD, PhD

Department of Neurosurgery

University of Utah

30 North 1900 East, Suite 3B409

Salt Lake City, UT 84132

Phone: 801-581-6908

Fax: 801-585-4385

Email: [william.couldwell@hsc.utah.edu](mailto:william.couldwell@hsc.utah.edu)

RUNNING HEAD: Celecoxib inhibits meningioma growth *in vivo*

KEY WORDS: meningioma, cyclooxygenase-2, COX-2, celecoxib, *in vivo*

TOTAL NUMBER OF PAGES: 30

TOTAL NUMBER OF TABLES: 0

TOTAL NUMBER OF ILLUSTRATIONS: 5

GRANTS: This work was supported by a grant from the American Association of Neurological Surgeons Neurosurgery Research and Education Foundation to B.R.

CONDENSED ABSTRACT: Celecoxib inhibits meningioma growth *in vivo* at plasma levels achievable in humans. COX-2 inhibitors may have a role in treatment of recurrent meningiomas.

**ABSTRACT**

**Background:** Treatments for recurrent meningiomas are limited. We previously demonstrated universal expression of COX-2 in meningiomas and dose-dependent growth inhibition *in vitro* with celecoxib, a COX-2 inhibitor. We therefore tested the effects of celecoxib on meningioma growth in a mouse xenograft model.

**Methods:** Meningioma cell lines (IOMM-Lee, CH157-MN, WHO grade I primary cultured tumor) were transplanted into flanks of nude mice fed mouse chow with celecoxib at varying concentrations (0, 500, 1000, 1500ppm) ad libitum. Tumors were measured biweekly and processed for MIB-1, Factor VIII, COX-2, and VEGF, and assayed with TUNEL.

**Results:** Celecoxib reduced growth of mean tumor volume by 66% ( $P<0.05$ ), 25% ( $P>0.05$ ), and 65% ( $P<0.05$ ) compared with untreated controls in IOMM-Lee, CH157-MN, and benign tumors, respectively. IOMM-Lee tumors removed from celecoxib treatment regained a growth rate similar to the control. Blood vessel density decreased and apoptotic cells increased in treated flank tumors. Diminished COX-2 expression and VEGF were observed in treated IOMM-Lee tumors. Mean plasma celecoxib levels were 845, 1540, and 2869ng/mL, for low-, medium-, and high-dose celecoxib, respectively.

**Conclusions:** Celecoxib inhibits meningioma growth *in vivo* at plasma levels achievable in humans. Celecoxib-treated tumors were less vascular with increased apoptosis.

IOMM-Lee tumors treated with celecoxib showed decreased COX-2 and VEGF expression. COX-2 inhibitors may have a role in treatment of recurrent meningiomas.

## INTRODUCTION

Meningiomas account for ~20% of all primary intracranial tumors, making them the second most common symptomatic adult central nervous system tumor.

Meningioma progression or recurrence may occur because of aggressive biology or unresectable location.<sup>1-3</sup> Recurrence rates for benign meningiomas five years after complete removal are only 2–3%, whereas recurrence rates for atypical and anaplastic meningiomas are 38–50% and 33–78%, respectively.<sup>4, 5</sup> Treatment options for recurrent meningiomas are limited.<sup>6, 7</sup> Radiation therapy is limited by side effects and tumor size, and systemic therapies have largely been disappointing.<sup>7-9</sup> Therefore, exploration of new treatment options is necessary.

The results of several head trauma epidemiologic studies have implicated the inflammatory process in meningoma pathogenesis.<sup>10</sup> Cyclooxygenase-2 (COX-2) is an inducible inflammatory response enzyme that is up-regulated in animal head trauma models.<sup>11</sup> Cyclooxygenase is the rate-limiting enzyme in the synthesis of prostaglandins from arachidonic acid.<sup>12</sup> Because prostaglandins are involved in various biologic activities, such as angiogenesis, increased cell proliferation, and suppression of apoptosis, interruption of this pathway may provide a therapeutic option in the treatment of recurrent meningiomas.

Overexpression of COX-2 has been closely linked to the tumorigenesis of colon, lung, and breast cancers.<sup>12, 13</sup> A growing body of literature supports the use of nonsteroidal anti-inflammatory drugs and selective COX-2 inhibitors in the treatment of an ever-widening number of cancers.<sup>14</sup> Previously, we demonstrated that COX-2 is universally expressed in meningiomas and that celecoxib, a selective COX-2 inhibitor,

inhibits meningioma growth *in vitro*, with evidence of apoptosis.<sup>15</sup> In this study, we investigated the effects of celecoxib on the growth of meningiomas in a mouse xenograft flank model.

## METHODS

### *Meningioma specimens*

A meningioma surgical specimen was obtained under Institutional Review Board-approved protocol and processed for cell culture. The tumor was graded as a WHO grade I meningioma,<sup>2</sup> which, for the purposes of this paper, we will describe as a primary cultured “benign meningioma.” This tumor specimen was grown as monolayer culture as described previously. Briefly, specimen was taken immediately from the operating room, digested in collagenase, and placed in Dulbecco’s Modified Eagle Medium (DMEM) (Sigma) supplemented with 10% fetal calf serum, L-glutamine (2 $\mu$ M), penicillin (50IU/mL), and streptomycin (50mg/mL). Cultured cells were maintained at 37°C in 7.5%CO<sub>2</sub>.

The human meningioma immortal cell lines IOMM-Lee and CH157-MN were also grown in DMEM supplemented with 10% fetal calf serum, L-glutamine (2 $\mu$ M), penicillin (50IU/mL), and streptomycin (50mg/mL) at 37°C in 7.5%CO<sub>2</sub>.<sup>16, 17</sup> The IOMM-Lee and CH157-MN cell lines were kind gifts from Dr. Ian McCutcheon (University of Texas, M.D. Anderson Cancer Center, Houston, Texas) and Dr. Yancey Gillespie (University of Alabama School of Medicine, Birmingham), respectively.<sup>16, 17</sup>

### *In vitro assays for COX-2 function*

To determine the effects of celecoxib treatment on the COX-2 enzyme, we analyzed IOMM-Lee cells grown in cell culture for COX-2 activity as well as cellular levels of prostaglandin E<sub>2</sub> (PGE<sub>2</sub>). IOMM-Lee cells were plated in T-175 flasks and allowed to grow to 75% confluence. Flasks were treated with vehicle control (0.1%DMSO) or 1.00mM celecoxib, as previously described.<sup>15</sup> Cells were harvested after 24h of treatment and protein was isolated. A total of four samples were processed for each treatment group.

Briefly, cells were rinsed with ice-cold Dulbecco's phosphate buffered saline, scraped from the culture dish, pelleted at 1,000g for 10min at 4°C, resuspended in 250µL of ice-cold buffer (0.1M Tris-HCl [pH7.8], containing 1mM ethylenediaminetetraacetic acid), and sonicated for 10sec three times. Cellular debris was pelleted by centrifugation at 10,000g at 4°C for 15min. The supernatant (nuclear and cytoplasmic) was removed and stored at -80°C until use. Samples were processed in triplicate for COX-2 activity (COX Activity Assay, Cayman Chemical Company, Ann Arbor, MI) and PGE<sub>2</sub> enzyme immunoassay (Prostaglandin E<sub>2</sub> EIA Kit-Monoclonal, Cayman Chemical Company) per the manufacturer's protocol.

#### *Meningioma mouse xenograft flank model*

All animal experiments were approved by the Animal Care and Use Committee of The University of Utah. Subcutaneous meningioma flank tumors were implanted as described previously.<sup>18</sup> Briefly, cells were grown to ~80% confluence in T-175 flasks. All steps were carried out on ice. The cells were rinsed with PBS, trypsinized, counted using a bright-line hemocytometer, pelleted at 1000rpm for 5min at 4°C, and

resuspended in media (IOMM-Lee and CH157-MN cell lines) or Matrigel (BD Biosciences, San Diego, CA) (primary meningioma cell line). Desired cell counts were 500,000 cells per mouse flank for the immortal cell lines and 5,000,000 per mouse flank for the primary meningioma cell line. A total volume of 0.10–0.15mL was injected subcutaneously into the flanks of immunodeficient mice (CD1, Charles River Laboratories, Wilmington, MA) using a tuberculin syringe and 25-gauge needle. Three-week-old mice were used for the dose-response experiments, whereas three-month-old mice were used for the prophylactic treatment experiments, as described below.

First, we performed dose-response experiments using 3-week-old mice and the IOMM-Lee cell line (control ( $n=20$ ); low-dose ( $n=10$ ), medium-dose ( $n=10$ ), high-dose ( $n=15$ ) celecoxib). Second, we repeated the high-celecoxib dosing regime with 3-week-old mice and both the CH157-MN cell line (control ( $n=10$ ), high-dose celecoxib ( $n=5$ )) and the benign cell line (control ( $n=5$ ), high-dose celecoxib ( $n=5$ )). Mice were sacrificed with a lethal intraperitoneal injection of pentobarbital. Flank tumors were excised, cut into blocks, and placed in 10% formalin for paraffin blocks or snap frozen in liquid nitrogen. Cardiac puncture was performed after euthanasia to obtain blood for celecoxib serum analysis.

#### *Treatment with celecoxib*

Celecoxib (G.D. Searle LLC, Chicago, IL) was included in mouse chow (Rodent Diet 8656, Harlan Teklad, Madison, WI) at 500 (low celecoxib), 1000 (medium), and 1500ppm (high). Tumors were allowed to grow for 10–14d before the initiation of treatment to allow the Matrigel or medium to resorb completely. The start of tumor

measurements was correlated with the initiation of the treatments. Control mice were fed regular mouse chow ad libitum. Treated mice were fed celecoxib mouse chow ad libitum. Mice in the prophylactic treatment groups were fed low-, medium-, or high-dose celecoxib for 6 weeks prior to subcutaneous flank injections and until sacrifice or the end of treatment.

#### *Analysis of celecoxib serum levels*

Following the sacrifice of the mice, whole blood was aspirated via cardiac puncture, placed into plasma separator tubes, and spun at 1,000rcf for 5min. The isolated plasma was placed into cryogenic tubes and stored at -80°C. Serum samples were shipped on dry ice to National Medical Services (Willow Grove, PA) for celecoxib serum analysis by high-performance liquid spectroscopy.

#### *Immunohistochemistry*

Immunohistochemistry analysis on formalin-fixed, paraffin-embedded meningoma mouse xenograft tumors was accomplished for MIB-1, Factor VIII, VEGF, and COX-2. Slides were cut at 4 microns, then melted at 55–60°C for 30min, deparaffinized in xylene for 5min, and rehydrated in graded alcohols (100%x2, 95%x2, 70%x1) for 1min each. The following steps were performed on the Ventana ES (Ventana Medical Systems, Tucson, AZ) at 40°C. Heat-induced epitope retrieval was accomplished by applying citrate buffer (pH6.0) in a microwave oven for 15min at half power and allowing it to cool for 15min for tissue stained for Factor VIII, VEGF, and COX-2. For the MIB-1 immunohistochemical staining, heat-induced epitope retrieval

was accomplished by applying citrate buffer (pH6.0) in an electric pressure cooker for 3min and allowing it to cool for 27min. The primary antibodies [Ki-67 (1:100, mouse monoclonal Ab, Clone MIB-1, Dako Cytomation, Carpinteria, CA), Factor VIII (1:1600, rabbit polyclonal Ab, Dako Cytomation), COX-2 (1:200, rabbit polyclonal, Lab Vision, Fremont, CA), or VEGF (1:200, mouse monoclonal, Dako Cytomation)] were applied for 32min followed by the appropriate secondary antibody [Mouse primary antibody: Mouse Fab (1:200, Mouse IgG, Dako Cytomation); rabbit primary antibody: Goat anti-mouse/anti-rabbit (1:300, Rabbit Fab, Dako Cytomation)] for 8min. Detection was done using the IView DAB detection kit (Ventana) and the counterstain was done with Hematoxylin (Ventana) for 4min. Slides were then dehydrated through graded alcohols (70%x1, 95%x2, 100%x2) for 30 seconds each, dipped in 4 changes of xylene, and covered with a coverslip. Positive controls consisted of pancreas tumor, normal tonsil, colon cancer, and normal colon for MIB-1, Factor VIII, COX-2, and VEGF, respectively. Negative controls were accomplished by running the above positive control tissue without the primary antibody.

#### *Apoptosis assay*

The terminal deoxynucleotidyl transferase-mediated dUTP nick-end labeling (TUNEL) technique was used to label the fragmented DNA of apoptotic cells. Formalin-fixed, paraffin-embedded mouse meningoma xenograft tumors were processed as recommended by the manufacturer (TUNEL Assay, Promega, Madison, WI), staining the fragmented DNA of apoptotic cells brown.

### *Immunohistochemical and apoptosis analysis*

Analysis of MIB-1 staining was performed by taking 6 random pictures per slide at 400x (10x ocular x 40x objective) using an Olympus Microfire camera. The images were analyzed using the Image-Pro Plus 5.0 graphic analysis program (Media Cybernetics, Silver Spring, MD). Results were reported as number of MIB-1 cells positive per 40x high-powered field (hpf) and represent the mean ( $\pm$ standard deviation) of 6 random fields. Three flank tumors were analyzed per treatment group, one slide per tumor.

Microvascular density analysis was achieved by scoring Factor VIII-stained slides, counting the number blood vessels positive in three 200x fields (10x ocular x 20x objective). Microscope fields were chosen based on the three fields with the maximal number of blood vessel stained (i.e., Factor VIII “hot-spots”), as described previously. Three flank tumors were analyzed per treatment group, one slide per tumor.

Immunohistochemical analysis for COX-2 and VEGF was accomplished by scoring 6 random fields per slide at 200x (10x ocular x 20x objective) for the percentage of cells stained and staining intensity. Areas of tumor necrosis and edge artifact were avoided. The percentage of cells stained was estimated to be 0%, 25%, 50%, 75%, or 100%. The intensity score was measured using a numerical scale (0 =no expression, 1+ =weak expression, 2+ =moderate expression, 3+ =strong expression.) A weight index was calculated [WI=% positive staining (>0) x intensity score]. Three flank tumors were analyzed per treatment group, one slide per tumor.

TUNEL staining for apoptosis was analyzed by counting the number of positively stained cells in 6 random fields per slide at 400x (10x ocular x 40x objective), avoiding areas of necrosis. Three flank tumors were analyzed per treatment group, one slide per tumor.

### *Statistical analysis*

*In vitro* data and immunohistochemical staining data (MIB-1, Factor 8, and TUNEL) were analyzed with the Student's t-test (unpaired, two-tailed t-test with confidence intervals set to 95%), whereas tumor growth curves and weighted immunohistochemical staining data (COX-2 and VEGF) were analyzed with one-way analysis of variance (one-way ANOVA, Tukey post-test with confidence intervals set to 95%) to compare control and treated groups, with statistical significance set at  $P < 0.05$ . Survival curves were analyzed with the  $\chi^2$  test, with statistical significance set at a  $P < 0.05$ . Statistics were analyzed using the GraphPad Prism 4.0 (San Diego, CA) statistical program.

## **RESULTS**

### *Celecoxib inhibits COX-2 activity and decreases PGE<sub>2</sub> concentrations in vitro*

The IOMM-Lee cell line was grown in culture, treated with 1.0mM celecoxib for 24h, and processed for COX-2 function to include the COX-2 activity assay and PGE<sub>2</sub> metabolite levels. Celecoxib completely inhibited mean ( $\pm$ SD) COX-2 activity *in vitro* with an overall reduction of 100% (2.9 $\pm$ 1.2U/mL vs. -0.1 $\pm$ 0.5U/mL; t-test  $P = 0.004$ )

(Figure 1). Correspondingly, cellular PGE<sub>2</sub> levels fell by 51% (50.9±21.5ng/mL vs. 24.9.1±10.3ng/mL; t-test  $P=0.003$ ) (Fig. 1).

#### *Meningioma flank tumor characteristics*

The IOMM-Lee immortal cell line was originally obtained from a 61-year-old man with an interosseous meningioma, WHO grade 3, in 1990.<sup>16</sup> The CH157-MN immortal cell line was originally obtained from a 55-year-old woman.<sup>17</sup> The WHO grade I tumor was a convexity, transitional meningoma, obtained from a 55-year-old man. All three meningiomas underwent Giemsa-band karyotype showing chromosomal abnormalities consistent with meningiomas (e.g., loss of chromosomes 1 and 22, as well as addition of chromosomes 1, 9q, 12q, 18, 20) (data not shown).<sup>2, 15, 19</sup> Histologically, flank tumors derived from IOMM-Lee and CH157-MN cell lines exhibited sheeting cytoarchitecture composed of large pleomorphic tumor cells. The benign cell line showed a cytoarchitecture vaguely resembling the original operative transitional meningioma subtype. Macroscopically, all three of these tumors exhibited a necrotic core with a peripheral ring of live tumor. Immunohistochemically, the IOMM-Lee, CH157-MN, and benign meningioma flank tumors were vimentin positive, epithelial membrane antigen positive, and glial fibrillary acid protein negative (data not shown). Transmission electron microscopy of the IOMM-Lee and CH157-MN flank tumors exhibited ultrastructural features consistent with meningiomas (e.g., intercellular junctions) (data not shown).<sup>20</sup> These features (i.e., karyotypic abnormalities, immunohistochemistry, and ultrastructural features) are typical of meningiomas.<sup>19-21</sup>

*Effect of celecoxib treatment on meningioma growth in vivo*

The results of dose-response experiments comparing the growth rate of IOMM-Lee tumors treated with low-, medium-, and high-dose celecoxib showed a trend toward a dose-dependent growth inhibition response (Fig. 2A). No statistically significant difference in tumor growth inhibition was found between the control and low- and medium-dose celecoxib treatment groups (ANOVA,  $P>0.05$ ), whereas the high-dose group showed statistically significant growth inhibition by day 43 (ANOVA,  $P<0.01$ ). Doubling time for the IOMM-Lee tumors in the control and high-dose treatment groups was ~2 and ~4 weeks, respectively. High-dose celecoxib treatment reduced the mean ( $\pm$ SD) tumor volume over control by 66% at 6 weeks ( $2821\pm 1907\text{mm}^3$  vs.  $948\pm 728\text{mm}^3$ , ANOVA,  $P<0.01$ ).

Based on the results from the IOMM-Lee dose-response experiments, we repeated the high-dose celecoxib treatment regime *in vivo* with the CH157-MN line and a benign meningioma mouse xenograft. The CH157-MN tumors in the control and high-dose celecoxib treatment groups doubled in ~6 and ~7d, respectively (Fig. 2B). Treatment reduced mean tumor volume by 25% by 6 weeks ( $3196\pm 257\text{mm}^3$  vs.  $2405\pm 1944\text{mm}^3$ , ANOVA,  $P>0.05$ ) The benign meningioma in the control and high-dose treatment groups doubled in ~2 weeks and ~5 weeks, respectively (Fig. 2C). Treatment reduced mean tumor volume by 65% by 5 weeks ( $5588\pm 3405\text{mm}^3$  vs.  $1966\pm 1685\text{mm}^3$ , ANOVA,  $P<0.05$ ). Statistically significant differences in tumor growth inhibition were noted between control and high-dose celecoxib treatment groups for the IOMM-Lee and benign meningioma flank tumors.

The IOMM-Lee, CH157-MN, and benign groups each showed 100% tumor induction (55/55, 15/15, and 10/10, respectively). The IOMM-Lee control group had one tumor that regressed in size (5%, 1/20).

Survival curves showed no statistically significant difference in the death rate between control and treated groups ( $\chi^2$  test,  $P>0.05$ , data not shown). Three of 20 control IOMM-Lee mice died, whereas none (0/10) in the low-dose group, none (0/10) in the medium-dose group, and two (2/15) mice in the high-dose celecoxib group died by day 43. No animals died in the CH157-MN tumor groups. One animal in the control benign meningioma flank tumor group died, and none (0/5) of the high-dose celecoxib group died by day 35.

#### *Celecoxib plasma levels*

Celecoxib serum levels obtained on sacrificed animals fed low-, medium-, and high-dose celecoxib mouse chow ad libitum for a minimum of 35d (i.e., drug levels reflect steady state) showed mean celecoxib plasma values ( $\pm$ SD) of 845( $\pm$ 267) ng/mL, 1540( $\pm$ 493) ng/mL, and 2869( $\pm$ 828) ng/mL, respectively (Fig. 3).

#### *Immunohistochemical staining and TUNEL results*

Immunohistochemistry was performed to analyze proliferative rates (MIB-1), microvascular density (Factor VIII), and COX-2 and VEGF expression in flank tumors treated with celecoxib. Immunohistochemical staining for the MIB-1 cell proliferative marker showed a slight increase in the mean number of cells positive in the IOMM-Lee flank tumors treated with high-dose celecoxib by 6% (211 $\pm$ 75 vs. 223 $\pm$ 64,  $P=0.627$ ) and

a significant increase of 14% ( $190 \pm 24$  vs.  $217 \pm 23$ ,  $P=0.005$ ) in the CH157-MN tumors (Fig. 4A). Conversely, the benign flank tumors treated with high-dose celecoxib showed a significant decrease in the mean number of MIB-1 positive cells by 21% ( $233 \pm 60$  vs.  $184 \pm 61$ , t-test,  $P=0.024$ , Fig. 4A,B).

Factor VIII microvascular density analysis showed a decrease in microvascular density of 22% (t-test,  $P=0.278$ ), 77% (t-test,  $P=0.009$ ), and 37% (t-test,  $P=0.015$ ) in the IOMM-Lee, CH157-MN, and benign flank tumors treated with high-dose celecoxib compared with the controls. Mean microvascular densities ( $\pm$ SD) per 20x hpf for the IOMM-Lee, CH157-MN, and benign flank tumors for control versus high-dose celecoxib treatment were  $4.9(\pm 2.8)$  versus  $3.8(\pm 0.8)$ ,  $5.2(\pm 1.2)$  versus  $1.2(\pm 0.4)$ , and  $5.1(\pm 1.4)$  versus  $3.2(\pm 1.5)$ , respectively (Fig. 4B).

The TUNEL apoptosis stain showed that treated groups had 36% (t-test,  $P=0.516$ ), 152% (t-test,  $P=0.002$ ), and 288% (t-test,  $P=0.022$ ) more cells undergoing apoptosis for IOMM-Lee, CH157-MN, and benign flank tumors treated with high-dose celecoxib than did the control groups. Mean TUNEL positive cells ( $\pm$ SD) per 40x hpf for the IOMM-Lee, CH157-MN, and benign flank tumors for control versus high-celecoxib treatment were  $1.4(\pm 1.8)$  versus  $1.9(\pm 2.0)$ ,  $1.3(\pm 1.5)$  versus  $3.2(\pm 1.9)$ , and  $0.8(\pm 0.9)$  versus  $3.1(\pm 3.4)$ , respectively (Fig. 4C).

Immunohistochemical staining for COX-2 and VEGF accomplished on IOMM-Lee xenograft tumors showed decreased staining scores with increasing celecoxib dose (Fig. 5A-C). Statistical significance was achieved for both COX-2 and VEGF at high-celecoxib dosing (ANOVA,  $P \leq 0.001$ ).

## DISCUSSION

The COX-2 enzyme is ubiquitously expressed in meningioma cells and also is present in endothelial cells, macrophages, and stromal tissues.<sup>15, 22-24</sup> Up-regulation of COX-2 contributes to tumor growth in cancer models by increasing angiogenesis and cellular proliferation, as well as decreasing apoptosis.<sup>14, 22-25</sup> Celecoxib, a selective COX-2 inhibitor, was chosen because of its FDA approval and has been shown to decrease cancer growth *in vitro* and *in vivo* by both COX-2–dependent and COX-2–independent mechanisms, making it difficult to ascertain whether drug effect is due to direct COX-2 inhibition.<sup>26, 27</sup> Regardless of the mechanism, we have demonstrated that celecoxib decreases meningioma growth *in vivo* with evidence of decreased microvascular density, increased apoptosis, and decreased COX-2 and VEGF expression. Celecoxib mouse serum levels for the low- and medium-dose regimes were well within reported ranges, whereas the high-dose regime, although achievable, is unrealistic in humans.

First, we showed that celecoxib eliminates COX-2 activity *in vitro*, corresponding with a 51% reduction in PGE<sub>2</sub> levels. Our previous *in vitro* work showed growth inhibition and apoptosis at similar celecoxib doses; however, it was unclear whether these findings were due to direct-COX-2 inhibition and subsequent reduction in prostaglandins or via other mechanisms.<sup>15</sup> These results fit with the extensive *in vitro* data on numerous cell lines showing growth inhibition by selective COX-2 inhibitors.<sup>15, 23, 28</sup> Specifically, another study on other brain tumors with the COX-2 inhibitor NS-398 showed inhibition of cell proliferation and migration of the glioma cell lines U-87MG and U-251MG.<sup>15, 29</sup>

We demonstrated a statistically significant decrease in meningioma mouse flank tumor sizes with high-dose celecoxib treatment in two of three cell lines, with a final mean tumor volume reduction between 25 and 66%. A trend toward a dose-dependent response was seen in one cell line grown in mice flanks, but it did not reach statistical significance for the low- or medium-dose celecoxib groups. Prophylactically treating mice with high-dose celecoxib for 6 weeks before induction of IOMM-Lee xenograft tumors resulted in decreased tumor induction rates compared to control, low-, and medium- dose groups (80% vs. 100%) (data not shown). Furthermore, removal of drug resulted in the return of tumor growth to baseline tumor growth rates, suggesting a tumor growth-suppressive of remaining viable cells (data not shown). These findings agree with those of other *in vivo* solid tumor studies (e.g., colorectal, prostate, lung, squamous cell carcinoma, breast) showing decreased tumor size with celecoxib treatment.<sup>30-36</sup>

Studies consistently show that selective COX-2 inhibitors reduce angiogenesis, probably via direct inhibition of the COX-2 enzyme.<sup>22-25</sup> COX-2 has been shown to regulate angiogenesis primarily through PGE<sub>2</sub>, which is a key regulator in stimulating VEGF expression.<sup>24, 25, 37, 38</sup> Furthermore, several *in vitro* studies show that COX-2 inhibitors down-regulate COX-2 expression.<sup>39, 40</sup> We verify these findings by showing that celecoxib reduced microvascular density in meningioma flank tumors by 23–78%. Furthermore, we provide evidence that COX-2 expression is diminished in celecoxib-treated meningioma flank tumors. Finally, we observe that VEGF expression is diminished, suggesting that celecoxib ultimately inhibits microvascular proliferation by inhibiting VEGF stimulation. Liu et al. showed that selective COX-2 inhibition

suppressed tumor growth through a down-regulation of a VEGF-mediated tumor angiogenesis.<sup>24</sup> Taken together, these results indicate that selective COX-2 inhibitors probably mediate their antiangiogenic effects via direct inhibition of the COX-2 enzyme (i.e., COX-2–dependent effect). Although we are unclear whether the antiangiogenic effects in this study are due to direct COX-2 inhibition, we provide evidence to support that this is the case.

Selective COX-2 inhibition has been shown to promote apoptosis in numerous cell lines *in vivo* and *in vitro*.<sup>22, 27, 38, 41, 42</sup> In this study, we have shown that celecoxib increases the number of cells undergoing programmed cell death by 36–288%. Although the specific antiapoptotic mechanism(s) remain unclear, proposed mechanisms include modulation of the BAX-to-bcl-2 ratio and activation of caspase pathways.<sup>13, 41, 42</sup> Previous *in vitro* work accomplished in our laboratory has shown no significant change in BAX or bcl-2 expression by Western blot analysis.<sup>15</sup> Thus, it appears that modulation of the BAX-to-bcl-2 ratio is not a factor in driving meningoma apoptosis *in vitro*, although we have not specifically studied this *in vivo*.

Celecoxib treatment of flank meningiomas resulted in slight increases in MIB-1 staining of the immortal meningoma cell lines (IOMM-Lee and CH157-MN). Conversely, flank tumors induced by the benign cell line showed a decrease in the number of cells undergoing cell division. This corresponds with the mixed results reported by others.<sup>24, 29, 36</sup> For example, the COX-2 inhibitor NS-398 inhibits cell proliferation and migration of the glioma cell lines U-87MG and U-251MG *in vitro*,<sup>29</sup> whereas others have shown no change in cell proliferation with selective COX-2 inhibition.<sup>24, 36</sup> Interestingly, because the MIB-1 antibody recognizes the Ki-67 nuclear antigen during G1, S, G2, and M

phases of the cell cycle, treatment with drugs that halt cells in G1 or the G1-S transition (beyond G0 but before S phase) can cause a paradoxical increase in labeling while still arresting cell growth.<sup>43</sup> This may explain our findings of increased Ki-67 labeling in the immortal cell lines flank tumors.

The recommended dose for celecoxib in the treatment of rheumatoid arthritis, osteoarthritis, and familial adenomatous polyposis ranges from 200 to 800mg a day, and for clinical trials doses up to 800mg a day have been reported. The plasma half-life of celecoxib is 13h, with steady state reached at 5d. Peak plasma levels of approximately 800ng/mL (~0.8µg/mL) have been observed after single 200-mg doses in healthy, fasting subjects.<sup>44</sup> Peak plasma levels of 1234µg/L (~1.2µg/mL) and 1160µg/L (~1.2µg/mL) have been observed an average of 3h after 300-mg single dose (mean) and at steady state, respectively, in 11 pediatric patients ages 6 to 15 being treated for solid tumors.<sup>45</sup> Frank et al. analyzed 35 adults taking celecoxib 400mg daily and reported a plasma concentration steady state of 600.61ng/mL (~0.6µg/mL) at 6 weeks.<sup>46</sup> Our *in vivo* celecoxib inclusion diets ranged from 500 to 1500ppm with mean plasma levels of 845ng/mL (~0.85µg/mL), 1540ng/mL (~1.4ng/mL), and 2869ng/mL (~2.9ng/mL) for the low-, medium- and high-dose celecoxib doses, respectively. Therefore, our low- and medium-dose celecoxib diets yield plasma levels within reported human ranges. Plasma levels of the high-dose celecoxib diet, although achievable in humans, would require ingestion of roughly 3 grams of celecoxib daily, which is not realistic (Pfizer, personal communication). Unlike other central nervous system tumors (e.g., astrocytomas) meningiomas derive their blood supply primarily from extracranial blood vessels, thus they are located outside the blood–brain barrier.

Therefore, intratumor drug concentrations from systemic therapies should mimic serum levels to a greater extent.

Celecoxib significantly inhibits meningioma growth *in vivo* at high plasma levels in this model. Overall, celecoxib-treated tumors were less vascular and had increased apoptosis than the control. IOMM-Lee tumors treated with celecoxib showed decreased COX-2 and VEGF expression. Interestingly, the tumor lines used in this study were highly aggressive, with areas of necrosis noted on histologic analysis. These findings are consistent with anaplastic meningiomas, perhaps making these findings more applicable to higher-grade tumors. COX-2 inhibitors may have a role in the treatment of recurrent meningiomas.

#### **ACKNOWLEDGMENTS**

We thank Kristin Kraus for her excellent editorial assistance, as well as David Kelly and Sheryl Tripp for their laboratory expertise. Finally, thanks to Dr. Peter Kan for his statistical assistance.

## REFERENCES

1. Burger PC, Scheithauer BW, Vogel FS, eds. *Surgical Pathology of the Nervous System and Its Coverings*. (4 ed). Philadelphia: Churchill Livingstone; 2002.
2. Louis DN, Scheithauer BW, Budka H, von Deimling A, Kepes JJ. Meningiomas. In: Kleihues P, Cavenee WK, eds. *World Health Organization Classification of Tumours: Pathology and Genetics: Tumours of the Nervous System*. Lyon: IARC Press; 2000.
3. Simpson D. The recurrence of intracranial meningiomas after surgical treatment. *J Neurol Neurosurg Psych*. 1957;20:22-39.
4. Mirimanoff RO, Dosoretz DE, Linggood RM, Ojemann RG, Martuza RL. Meningioma: analysis of recurrence and progression following neurosurgical resection. *J Neurosurg*. 1985;62:18-24.
5. Jaaskelainen J, Haltia M, Servo A. Atypical and anaplastic meningiomas: radiology, surgery, radiotherapy, and outcome. *Surg Neurol*. 1986;25:233-242.
6. Milosevic MF, Frost PJ, Laperriere NJ, Wong CS, Simpson WJ. Radiotherapy for atypical or malignant intracranial meningioma. *Int J Radiat Oncol Biol Phys*. 1996;34:817-822.
7. Rosenthal MA, Ashley DL, Cher L. Treatment of high risk or recurrent meningiomas with hydroxyurea. *J Clin Neurosci*. 2002;9:156-158.
8. Barnett GH, Suh JH, Crownover RL. Recent advances in the treatment of skull base tumors using radiation. *Neurosurg Clin N Am*. 2000;11:587-596.

9. Blankenstein MA, Verheijen FM, Jacobs JM, Donker TH, van Duijnhoven MW, Thijssen JH. Occurrence, regulation, and significance of progesterone receptors in human meningioma. *Steroids*. 2000;65:795-800.
10. Phillips LE, Koepsell TD, van Belle G, Kukull WA, Gehrels JA, Longstreth WT, Jr. History of head trauma and risk of intracranial meningioma: population-based case-control study. *Neurology*. 2002;58:1849-1852.
11. Kunz T, Marklund N, Hillered L, Oliw EH. Cyclooxygenase-2, prostaglandin synthases, and prostaglandin H2 metabolism in traumatic brain injury in the rat. *J Neurotrauma*. 2002;19:1051-1064.
12. Prescott SM. Is cyclooxygenase-2 the alpha and the omega in cancer? *J Clin Invest*. 2000;105:1511-1513.
13. Umar A, Viner JL, Anderson WF, Hawk ET. Development of COX inhibitors in cancer prevention and therapy. *Am J Clin Oncol*. 2003;26:S48-57.
14. Hinz B, Brune K. Cyclooxygenase-2--10 years later. *J Pharmacol Exp Ther*. 2002;300:367-375.
15. Ragel BT, Jensen RL, Gillespie DL, Prescott SM, Couldwell WT. Ubiquitous expression of cyclooxygenase-2 in meningiomas and decrease in cell growth following in vitro treatment with the inhibitor celecoxib: potential therapeutic application. *J Neurosurg*. 2005;103:508-517.
16. Lee WH. Characterization of a newly established malignant meningioma cell line of the human brain: IOMM-Lee. *Neurosurgery*. 1990;27:389-395; discussion 396.

17. Tsai JC, Goldman CK, Gillespie GY. Vascular endothelial growth factor in human glioma cell lines: induced secretion by EGF, PDGF-BB, and bFGF. *J Neurosurg.* 1995;82:864-873.
18. Jensen RL, Leppla D, Rokosz N, Wurster RD. Matrigel augments xenograft transplantation of meningioma cells into athymic mice. *Neurosurgery.* 1998;42:130-135; discussion 135-136.
19. Ragel BT, Jensen RL. Molecular genetics of meningiomas. *Neurosurg Focus.* 2005;19:E9.
20. Akat K, Mennel HD, Kremer P, Gassler N, Bleck CK, Kartenbeck J. Molecular characterization of desmosomes in meningiomas and arachnoidal tissue. *Acta Neuropathol (Berl).* 2003;106:337-347.
21. Rutka JT, Giblin J, Dougherty DV, McCulloch JR, DeArmond SJ, Rosenblum ML. An ultrastructural and immunocytochemical analysis of leptomeningeal and meningioma cultures. *J Neuropathol Exp Neurol.* 1986;45:285-303.
22. Williams CS, Tsujii M, Reese J, Dey SK, DuBois RN. Host cyclooxygenase-2 modulates carcinoma growth. *J Clin Invest.* 2000;105:1589-1594.
23. Tsujii M, Kawano S, Tsuji S, Sawaoka H, Hori M, DuBois RN. Cyclooxygenase regulates angiogenesis induced by colon cancer cells. *Cell.* 1998;93:705-716.
24. Liu XH, Kirschenbaum A, Yao S, Lee R, Holland JF, Levine AC. Inhibition of cyclooxygenase-2 suppresses angiogenesis and the growth of prostate cancer in vivo. *J Urol.* 2000;164:820-825.

25. Reddy BS, Hirose Y, Lubet R, et al. Chemoprevention of colon cancer by specific cyclooxygenase-2 inhibitor, celecoxib, administered during different stages of carcinogenesis. *Cancer Res.* 2000;60:293-297.
26. Kardosh A, Blumenthal M, Wang WJ, Chen TC, Schonthal AH. Differential effects of selective COX-2 inhibitors on cell cycle regulation and proliferation of glioblastoma cell lines. *Cancer Biol Ther.* 2004;3:55-62.
27. Yamazaki R, Kusunoki N, Matsuzaki T, Hashimoto S, Kawai S. Selective cyclooxygenase-2 inhibitors show a differential ability to inhibit proliferation and induce apoptosis of colon adenocarcinoma cells. *FEBS Lett.* 2002;531:278-284.
28. King JG, Jr., Khalili K. Inhibition of human brain tumor cell growth by the anti-inflammatory drug, flurbiprofen. *Oncogene.* 2001;20:6864-6870.
29. Joki T, Heese O, Nikas DC, et al. Expression of cyclooxygenase 2 (COX-2) in human glioma and in vitro inhibition by a specific COX-2 inhibitor, NS-398. *Cancer Res.* 2000;60:4926-4931.
30. Fife RS, Stott B, Carr RE. Effects of a selective cyclooxygenase-2 inhibitor on cancer cells in vitro. *Cancer Biol Ther.* 2004;3:228-232.
31. Hsu AL, Ching TT, Wang DS, Song X, Rangnekar VM, Chen CS. The cyclooxygenase-2 inhibitor celecoxib induces apoptosis by blocking Akt activation in human prostate cancer cells independently of Bcl-2. *J Biol Chem.* 2000;275:11397-11403.
32. Klenke FM, Gebhard MM, Ewerbeck V, Abdollahi A, Huber PE, Sckell A. The selective Cox-2 inhibitor Celecoxib suppresses angiogenesis and growth of

- secondary bone tumors: an intravital microscopy study in mice. *BMC Cancer*. 2006;6:9.
33. Kundu N, Fulton AM. Selective cyclooxygenase (COX)-1 or COX-2 inhibitors control metastatic disease in a murine model of breast cancer. *Cancer Res*. 2002;62:2343-2346.
  34. Sinicropo FA, Gill S. Role of cyclooxygenase-2 in colorectal cancer. *Cancer Metastasis Rev*. 2004;23:63-75.
  35. Srinath P, Rao PN, Knaus EE, Suresh MR. Effect of cyclooxygenase-2 (COX-2) inhibitors on prostate cancer cell proliferation. *Anticancer Res*. 2003;23:3923-3928.
  36. Zhang X, Chen ZG, Choe MS, et al. Tumor growth inhibition by simultaneously blocking epidermal growth factor receptor and cyclooxygenase-2 in a xenograft model. *Clin Cancer Res*. 2005;11:6261-6269.
  37. Cheng T, Cao W, Wen R, Steinberg RH, LaVail MM. Prostaglandin E2 induces vascular endothelial growth factor and basic fibroblast growth factor mRNA expression in cultured rat Muller cells. *Invest Ophthalmol Vis Sci*. 1998;39:581-591.
  38. Liu XH, Kirschenbaum A, Lu M, et al. Prostaglandin E2 induces hypoxia-inducible factor-1alpha stabilization and nuclear localization in a human prostate cancer cell line. *J Biol Chem*. 2002;277:50081-50086.
  39. Pai R, Soreghan B, Szabo IL, Pavelka M, Baatar D, Tarnawski AS. Prostaglandin E2 transactivates EGF receptor: a novel mechanism for promoting colon cancer growth and gastrointestinal hypertrophy. *Nat Med*. 2002;8:289-293.

40. Ferrandina G, Ranelletti FO, Legge F, et al. Celecoxib modulates the expression of cyclooxygenase-2, ki67, apoptosis-related marker, and microvessel density in human cervical cancer: a pilot study. *Clin Cancer Res.* 2003;9:4324-4331.
41. Cui W, Yu CH, Hu KQ. In vitro and in vivo effects and mechanisms of celecoxib-induced growth inhibition of human hepatocellular carcinoma cells. *Clin Cancer Res.* 2005;11:8213-8221.
42. Fosslien E. Biochemistry of cyclooxygenase (COX)-2 inhibitors and molecular pathology of COX-2 in neoplasia. *Crit Rev Clin Lab Sci.* 2000;37:431-502.
43. Couldwell WT, Weiss MH, Law RE, Hinton DR. Paradoxical elevation of Ki-67 labeling with protein kinase inhibition in malignant gliomas. *J Neurosurg.* 1995;82:461-468.
44. Karim A, Isakson P, Hubbard RC. Selective COX-2 inhibitor SC-58635: first in man administration and pharmacokinetic assessment. *8th APLAR Congress of Rheumatology.* 1996;108:5-6.
45. Stempak D, Gammon J, Klein J, Koren G, Baruchel S. Single-dose and steady-state pharmacokinetics of celecoxib in children. *Clin Pharmacol Ther.* 2002;72:490-497.
46. Frank DH, Roe DJ, Chow HH, et al. Effects of a high-selenium yeast supplement on celecoxib plasma levels: a randomized phase II trial. *Cancer Epidemiol Biomarkers Prev.* 2004;13:299-303.

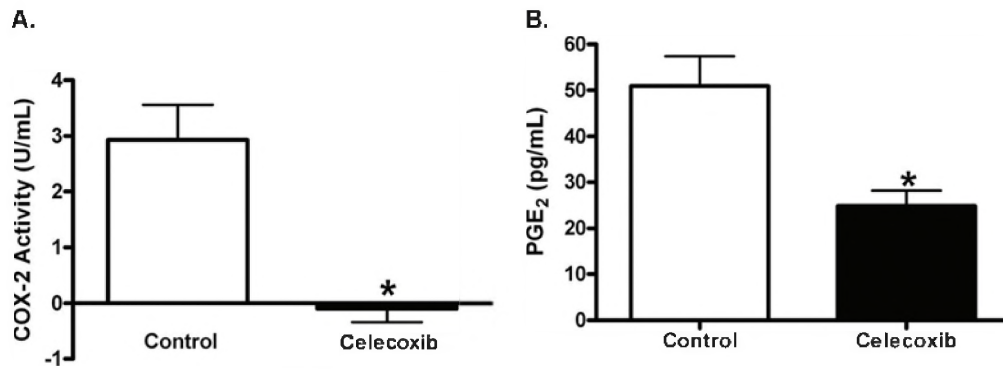


Figure 1: Graphs of COX-2 activity and PGE<sub>2</sub> enzyme immunoassay in IOMM-Lee cells treated with 1.0mM celecoxib *in vitro* for 24h. Error bars represent four samples per group analyzed in triplicate. A. COX-2 activity was completely suppressed with a decrease of 100% in IOMM-Lee cells treated with 1.0mM celecoxib for 24h (t-test, \* $P=0.004$ ). B. PGE<sub>2</sub> was decreased by 51% in treated cells vs. control (t-test, \* $P=0.003$ ).

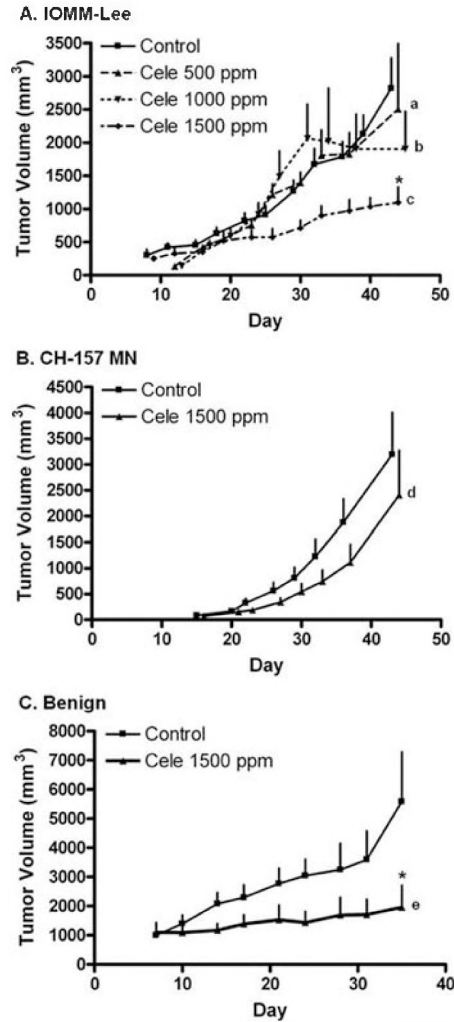


Figure 2: Celecoxib inhibits the growth of meningioma xenograft tumors. A. IOMM-Lee flank tumors show a dose-dependent growth inhibition with increasing doses of celecoxib. Control mice were fed regular mouse chow. Treated mice were fed low-, medium-, or high-dose celecoxib diets (500, 1000, and 1500 ppm, respectively). No statistically significant difference was found between the control and low (<sup>a</sup>ANOVA,  $P>0.05$ )- or medium (<sup>b</sup>ANOVA,  $P>0.05$ )-dose celecoxib treatment groups, whereas a statistically significant difference between the control and high-dose celecoxib groups was noted by day 43 (<sup>c</sup>ANOVA,  $P<0.05$ ). Error bars represent 20, 10, 10, and 15 mice for the control, low-, medium-, and high-celecoxib groups, respectively. B. CH157-MN

flank tumors treated with control and high-dose celecoxib. Error bars represent 10 and 5 mice, respectively. No statistical difference was noted between groups (<sup>d</sup>ANOVA,  $P>0.05$ ). C. Benign meningioma from operative specimen treated with control or high-dose celecoxib. A statistical difference was noted between groups by day 43 (<sup>e</sup>ANOVA,  $P<0.05$ ). Error bars represent 5 mice.

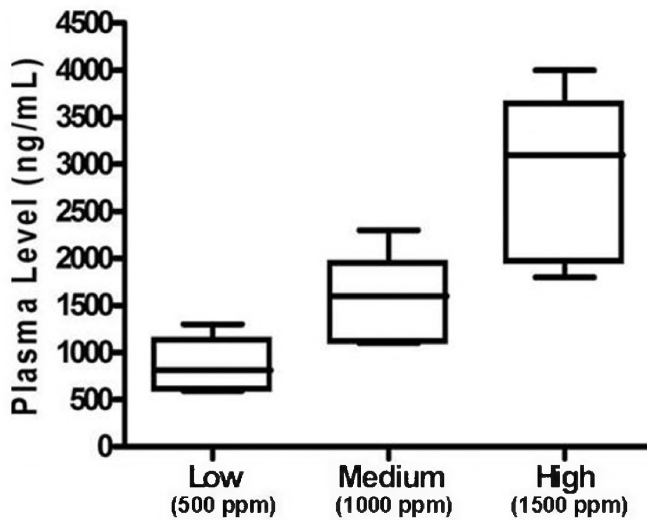


Figure 3. Celecoxib serum levels in animals fed low-, medium-, and high-dose celecoxib (500, 1000, and 1500 ppm, respectively) mouse chow ad libitum for a minimum of 35d (i.e., drug levels reflect steady state). Mean celecoxib plasma values ( $\pm$ SD) for low-, medium-, and high-dose celecoxib are 845( $\pm$ 267), 1540( $\pm$ 493), and 2869( $\pm$ 828)ng/mL, respectively.

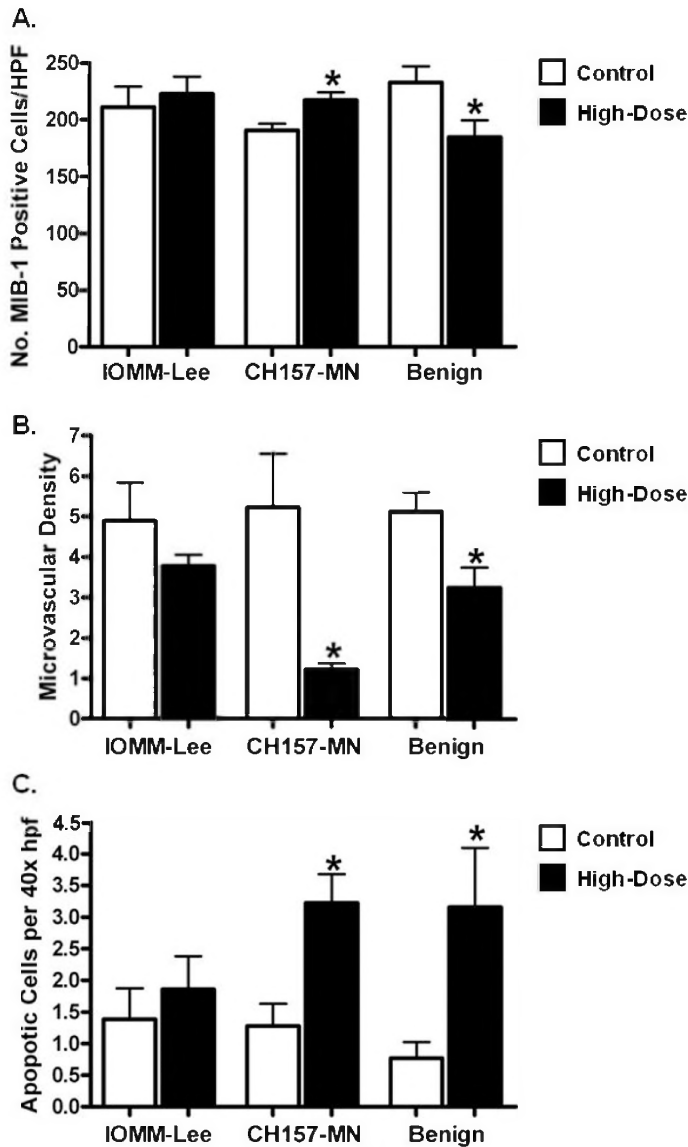


Figure 4: A–C: Bar graphs showing the number of MIB-1 positive cells (A), Factor VIII microvascular staining (B), and the number of TUNEL positive cells (C) in meningiomas grown in the mouse xenograft flank model for mice fed either regular mouse chow or high-dose (1500 ppm) celecoxib chow ad libitum. A. Proliferative rates for the IOMM-Lee and CH157-MN tumors showed a slight increase in proliferative cells when treated with celecoxib, whereas the benign flank tumors showed a statistically significant decrease in the number of MIB-1 positive cells when compared with the control (t-test,

\* $P=0.024$ ). B. Microvascular analysis of treated flank tumors showed a decrease in microvascular density when compared with control tumors, with statistical difference found in the CH157-MN (*t-test*, \* $P=0.009$ ) and the benign flank tumors (*t-test*, \* $P=0.015$ ). C. TUNEL assay of treated groups showed an apparent increase in the number of cells undergoing apoptosis, with statistical significance reached in the CH-157 and benign flank tumors (*t-test*, \* $P=0.002$  and \* $P=0.022$ , respectively).

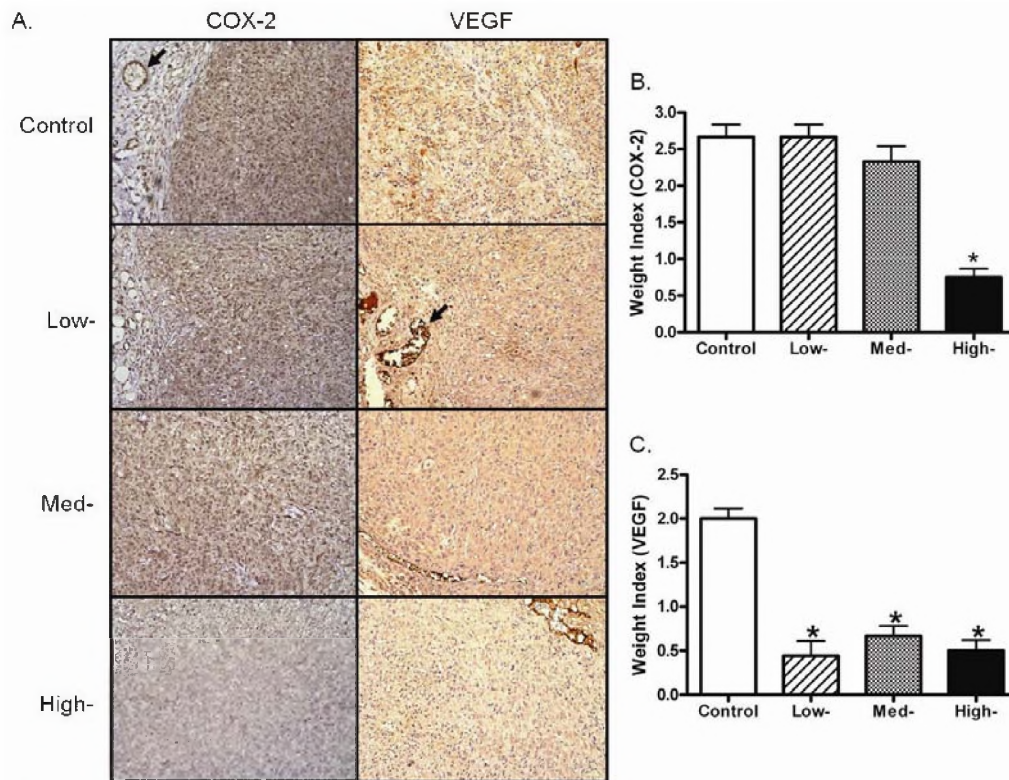


Figure 5: A. Representative pictures of COX-2 and VEGF immunohistochemical staining of IOMM-Lee xenograft tumors fed low-, medium-, and high-dose celecoxib (500, 1000, and 1500 ppm, respectively) mouse chow ad libitum for 43d. Magnification is 200X. Decreased COX-2 and VEGF staining intensity was noted as celecoxib dose increased. Arrows identify internal positive controls; both COX-2 and VEGF stain vascular

endothelium. B–C. Weighted index of COX-2 (B) and VEGF (C) staining showing a decrease in score with increasing celecoxib dose. Statistical significance achieved for both COX-2 and VEGF (ANOVA,  $*P<0.001$ ).